Supporting Information

Yamashita et al. 10.1073/pnas.0903699106

SI Materials and Methods

Cell Culture. The insect cell lines Sf9 and BTI-Tn-5B1–4 (Tn5) were maintained in Sf-900II medium (Invitrogen) supplemented with 10% FBS and Ex-cell 405 medium (JRH Biosciences), respectively. The human hepatoma cell lines, Huh7, PLC/PRF/5, HepG2, Hep3B, and FLC4, human alveolar epithelial A549 cells, and human embryonic kidney 293T cells were maintained in Dulbecco's modified Eagle's MEM (Sigma) supplemented with 10% FBS. Mouse myeloma P3U1 cells were grown in RPMI-1640 medium (Invitrogen) supplemented with 10% FBS.

Production of Anti-HEV-LP Monoclonal Antibodies. Hybridoma cells producing anti-HEV-LP monoclonal antibodies were generated at Bio Matrix Research by the standard method. All of 11 monoclonal antibodies (IgG1 or IgG2a isotypes) were confirmed to be capable of detecting HEV-LP on ELISA. These antibodies were purified by an affinity chromatography using protein G columns. Among them, MAB358, MAB1323, and MAB272 were biotinylated for use in the neutralization of cell-binding assay and competitive ELISA.

Expression of HEV Capsid Protein and Purification of HEV-LP. The recombinant baculovirus AcMNPV encoding amino acid residues 112 to 608 of the ORF2 of the HEV genotype 3, 2712 strain was produced by a Bacmid-based method (Invitrogen) following the manufacturer's instructions. To prepare a series of mutants of the HEV capsid protein in which asparagine was replaced with alanine at the residue 200 (N200A), or tyrosine was replaced with other amino acids at residue 288 (Y288A, Y288W, Y288F, Y288L, Y288D, Y288H, and Y288R), or surface amino acids of the P domain were replaced with alanines, the corresponding nucleotide mutations were introduced into pFastBac1 vector (Invitrogen) encoding the wild-type HEV ORF2 by a site-directed mutagenesis based on PCR (1). The virus stock was propagated in Sf9 cells and HEV-LP was expressed in Tn5 cells. HEV-LP was purified and particle formation was determined by a discontinuous sucrose gradient centrifugation as described previously (2). For immunoprecipitation and cell-binding analyses, the HEV-LP-containing fractions were dialyzed with PBS and concentrated to 200 μg/mL.

Crystallization of HEV-LP. Crystallizations were performed using the hanging-drop vapor-diffusion method at 293 K using the conditions described previously (3). The best crystals of HEV-LP were obtained with 6% (wt/vol) PEG 10,000 and 35% (wt/vol) ethylene glycol in 100 mM Tris-HCl buffer (pH 8.0). The droplets consisted of equal volumes (3 μL) of protein solution and reservoir solution.

Data Collection and Processing. The crystals of HEV-LP were mounted in nylon CryoLoops (Hampton Research) and placed directly into a nitrogen stream at 100 K. X-ray diffraction data were collected at 100 K on beamlines BL17A (wavelength 1.0000 Å) at the Photon Factory (KEK) using an ADSC Quantum 270 CCD detector. Oscillation data were recorded in frames of 0.3 oscillation with 30-s exposure time per image. The complete data set was merged with 3 crystal data sets. The collected data were processed with the program *HKL-2000* (4). The statistics of X-ray diffraction data collection are summarized in Table 1. The space groups of HEV-LP crystals were determined to be orthorhombic $P2_12_12_1$. Assuming the presence of 1 molecule of HEV-LP in the asymmetric unit, the value of the Matthews coefficient V_M (5) was 3.31 Å^3 Da^{-1}, corresponding to a solvent content of 62.8%, both of which were within the normal range of values for protein crystals (5). The self-rotation functions showed pronounced peaks indicating 2-fold, 3-fold, and 5-fold noncrystallographic rotation symmetry. The calculation of the Matthews coefficient is based on the reasonable assumption of a T = 1 particle.

Phase Determination. The self-rotation function was computed with the program *POLARRFN* of the *CCP4* package (6) to determine the orientation of icosahedral noncrystallographic symmetry elements. The particle orientation in the unit cell and particle position were determined by a self-rotation function and translation search with the crystal structure of HEV-LP genotype 1 which was previously determined at 8.3-Å resolution (3), respectively. By using the data in the range of 50–20-Å resolution, the maximum correlation coefficient and the minimum *R*-factor values were determined as 0.642 and 0.363, respectively. The particle orientation and position of HEV-LP of genotype 3 in the crystal were slightly different from those of genotype 1 (3), which resulted in the different length of the cell axes with the same space group ($P2_12_12_1$). Phase refinement and extension were carried out to the resolution of 3.5 Å as described previously (3). The final correlation coefficient and *R*-factor between the F_os and the F_cs obtained from inversion of the averaged and solvent-flattened map at 3.5 Å resolution were 0.928 and 0.235, respectively. The electron density map was of good quality and allowed interpretation in terms of the secondary and tertiary structures of the subunits. We built an atomic model into the electron density map using the program O (7), and the model was refined using the program CNS. We calculated the electrostatic potentials of HEV-LP by the *GRASP* program (7). The solved 3D structure of HEV-LP was submitted to the Protein Data Bank under the PDB accession code of 2ZTN.

Cell-Binding Assay. Cultured cells (5×10^5 cells)were detached with 2 mM EDTA and incubated with 100 μL HEV-LP (10 μg/mL) for 1 h at 4°C. After being washed twice with PBS containing 0.35% BSA, the cells were fixed with 0.5% paraformaldehyde for 15 min at 4°C. After further washing, HEV-LPs bound to cells were stained with anti-HEV-LP MAB358 and Alexa Flour 488-labeled goat anti-mouse IgG antibodies (Invitrogen), and analyzed by a BD FACSCalibur flow cytometry system (BD). For neutralization of binding of HEV-LP to cells, 100 μL HEV-LP (10 μg/mL) was preincubated with anti-HEV-LP monoclonal antibodies (20 μg/mL) for 1 h at 37°C before incubation with cells, and bound HEV-LPs were stained with biotinylated MAB358 and phycoerythrin-conjugated streptavidin (BD PharMingen).

Immunoprecipitation. The wild-type and mutant HEV-LPs (200 ng/mL) were incubated with Protein G Sepharose 4 Fast Flow beads (GE Healthcare) for 1 h at 4°C. After centrifugation, 0.5 μg anti-HEV-LP monoclonal antibodies were added to the supernatants. After incubation for 1 h at 4°C, 15 μL Protein G beads was added and the solution was further incubated for 1 h at 4°C. The beads were washed 5 times with PBS containing 0.5% Tween20, suspended in 30 μL SDS/PAGE sample buffer and boiled for 5 min. The samples were analyzed by western blotting using an anti-HEV-LP rabbit polyclonal antibody.

1. Higuchi R, Krummel B, Saiki RK (1988) A general method of in vitro preparation and specific mutagenesis of DNA fragments: Study of protein and DNA interactions. *Nucleic Acids Res* 16:7351–7367.
2. Xing L, *et al.* (1999) Recombinant hepatitis E capsid protein self-assembles into a dual-domain T = 1 particle presenting native virus epitopes. *Virology* 265:35–45.
3. Wang CY, *et al.* (2008) Crystallization and preliminary X-ray diffraction analysis of recombinant hepatitis E virus-like particle. *Acta Crystallogr Sect F Struct Biol Cryst Commun* 64:318–322.
4. Otwinowski Z, Minor W (1997) Processing of X-ray diffraction data collected in oscillation mode. *Methods in Enzymology* 276:307–326.
5. Matthews BW (1968) Solvent content of protein crystals. *J Mol Biol* 33:491–497.
6. Collaborative Computational Project N (1994) The CCP4 suite: Programs for protein crystallography. *Acta Crystallogr D Biol Crystallogr* 50:760–763.
7. Nicholls A, Sharp KA, Honig B (1991) Protein folding and association: Insights from the interfacial and thermodynamic properties of hydrocarbons. *Proteins* 11:281–296.

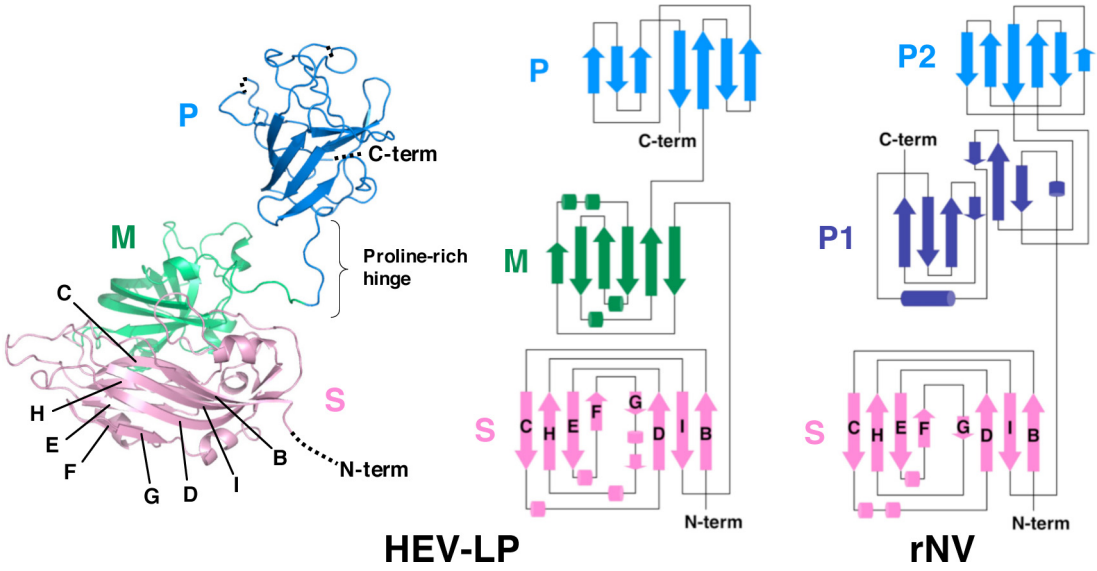

Fig. S1. Capsid monomers of HEV-LP and rNV. The ribbon diagram of a capsid monomer of HEV-LP is indicated in the left. The respective topology diagrams of capsid monomers from HEV-LP and recombinant Norwalk virus (rNV) are indicated. The S, M, and P domains of the HEV-LP capsid protein are indicated by pink, green and blue, respectively. The S, P1, and P2 domains of the rNV capsid protein are indicated by pink, dark blue, and blue, respectively. The β-strands and α-helices are shown with arrows and tubes, respectively.

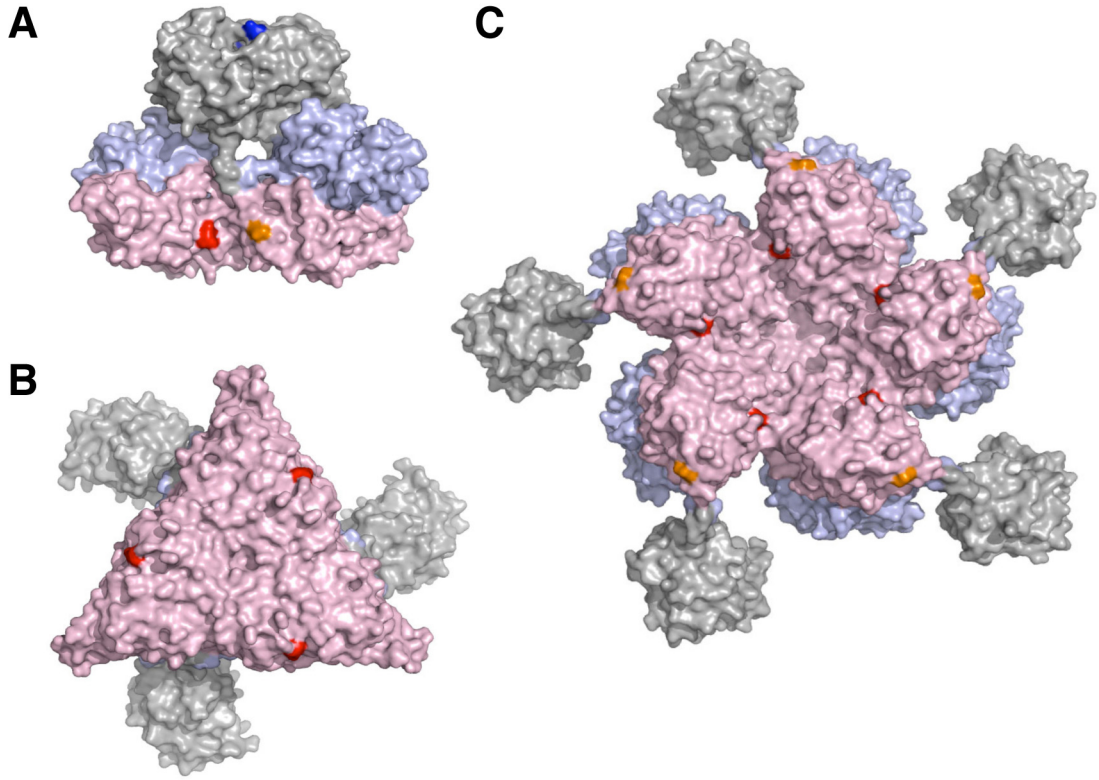

Fig. S2. Three-dimensional mapping of potential *N*-glycosylation sites at dimer (*A*), trimer (*B*), and pentamer (*C*) structures of the capsid protein in HEV-LP. Asparagine residues of possible *N*-glycosylation sites, Asn-137-Leu-Ser, Asn-310-Leu-Thr, and Asn-562-Thr-Thr, are colored red, orange, and blue, respectively, on the surface diagrams from a lateral (*A*) or inside (*B* and *C*) view. The S, M, and P domains are indicated in pink, blue, and gray, respectively.

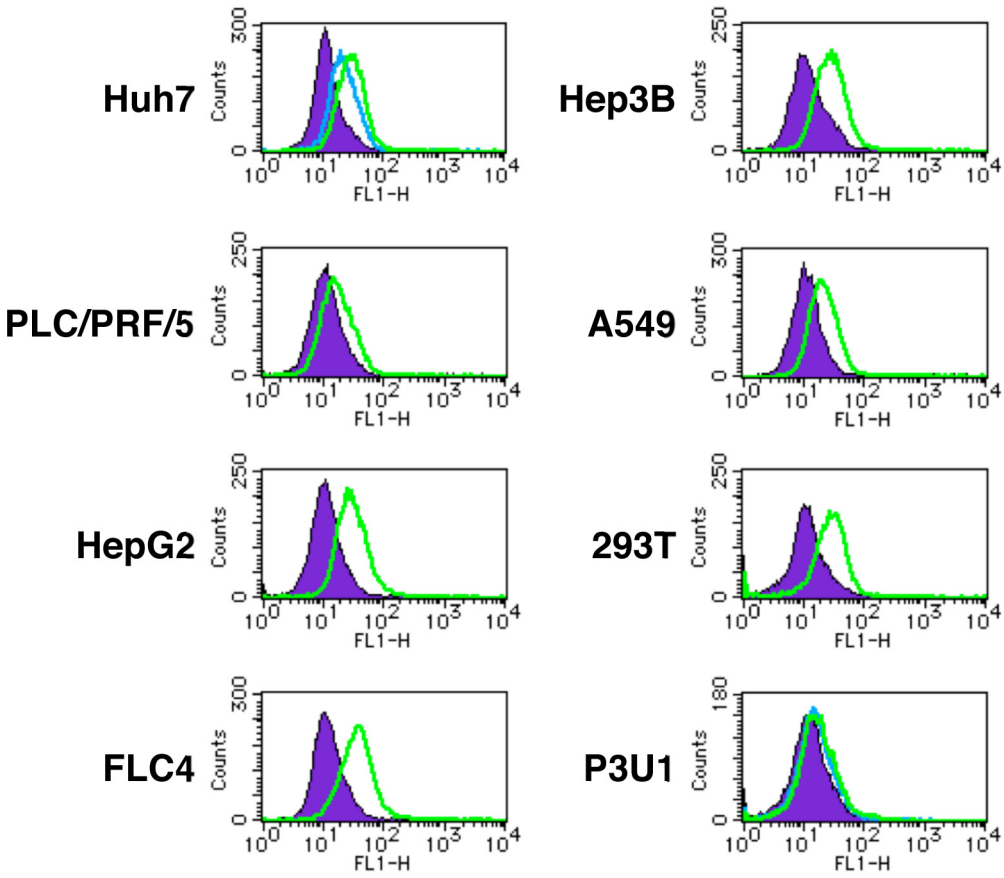

Fig. S3. HEV-LP binding to culture cells. HEV-LPs were incubated with the indicated cells for 1 h at 4°C, and then HEV-LPs bound to cells were detected by flow cytometry. The blue and green lines indicate incubation with 1 and 10 μg/mL HEV-LPs, respectively. The filled area indicates mock-incubated cells.

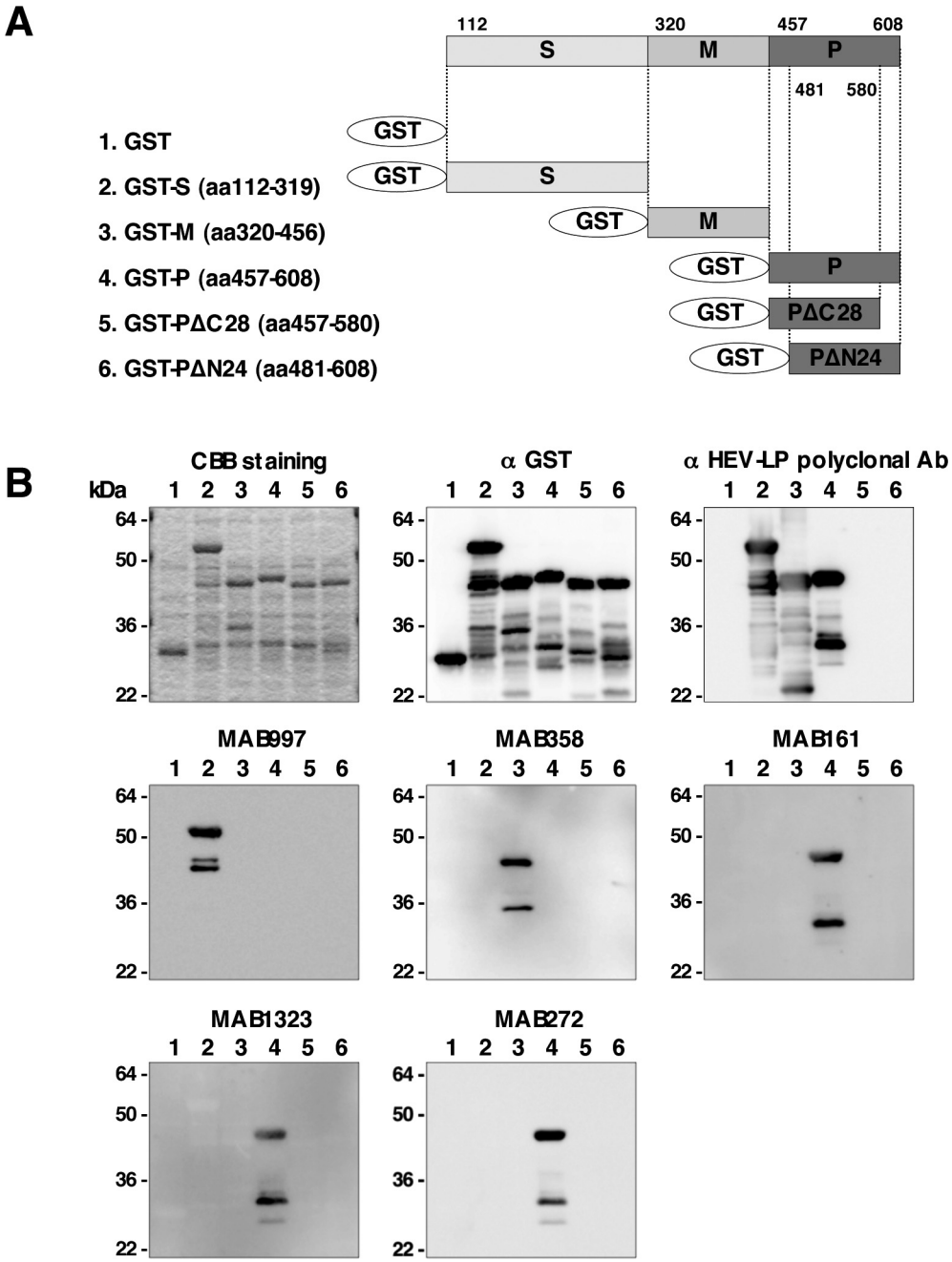

Fig. S4. Determination of HEV-LP subdomain recognized by anti-HEV-LP antibodies. (*A*) Schematic representation of GST or GST-fused HEV-LP subdomains used for epitope mapping. The cDNAs encoding the indicated amino acid residues were introduced into a pGEX-4T3 vector and were expressed as GST-fused proteins in bacteria. (*B*) The lysates of cells expressing GST or GST-fused proteins were applied to SDS/PAGE and stained with Coomassie Brilliant Blue (CBB) or examined by immunoblotting with polyclonal and monoclonal antibodies. The lane numbers correspond to those in *A*.

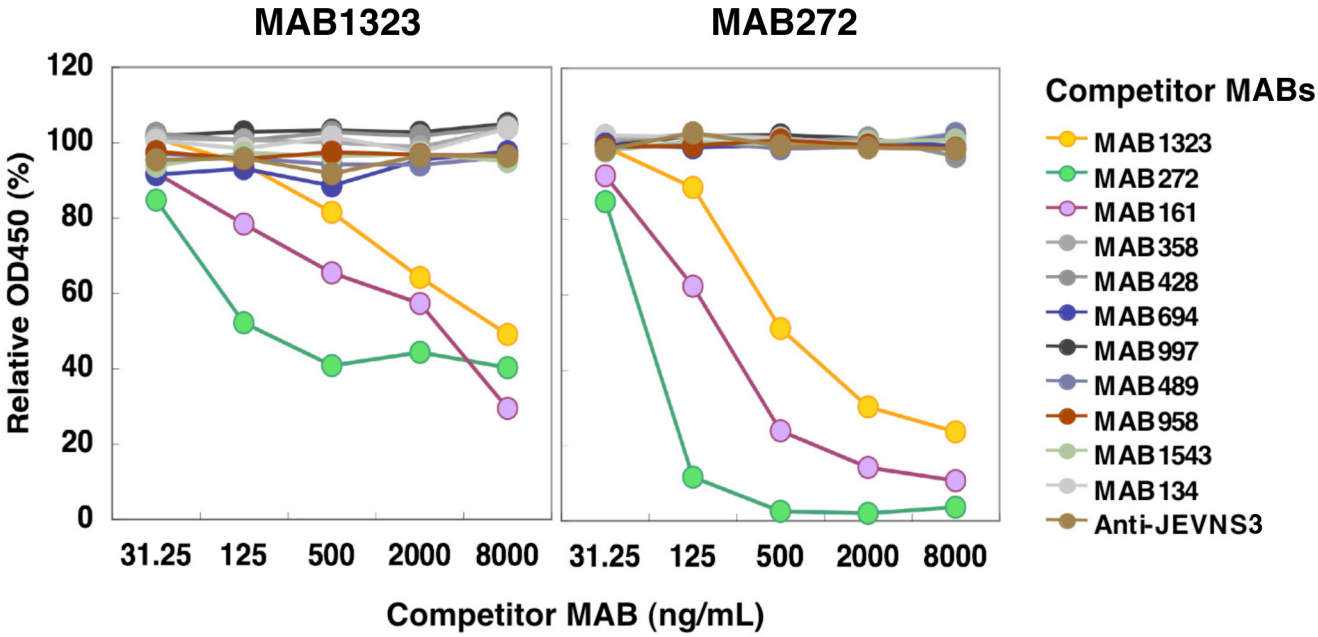

Fig. S5. Competitive ELISA of monoclonal antibodies to HEV-LP. The wild-type HEV-LP (50 or 100 ng/mL) was inoculated into wells of a 96-well-immuno-plate (Nunc) and incubated at 4°C overnight. Unbound HEV-LP was washed out with PBST 3 times and the wells were incubated with PBS containing 1% BSA. After washing, serially diluted competitor antibodies were reacted for 1 h at 25°C. After washing 5 times, biotinylated MAB1323 (500 ng/mL) or MAB272 (50 ng/mL) was reacted for 1 h at 25°C. Bound biotinylated antibodies were further reacted with horseradish peroxidase-conjugated streptavidin (Vector) and visualized with 3, 3′, 5, 5′-tetramethyl-benzidene (Nacalai Tesque). Optical densities of 450 nm in the wells without competitor antibodies were defined as 100% reactivity.

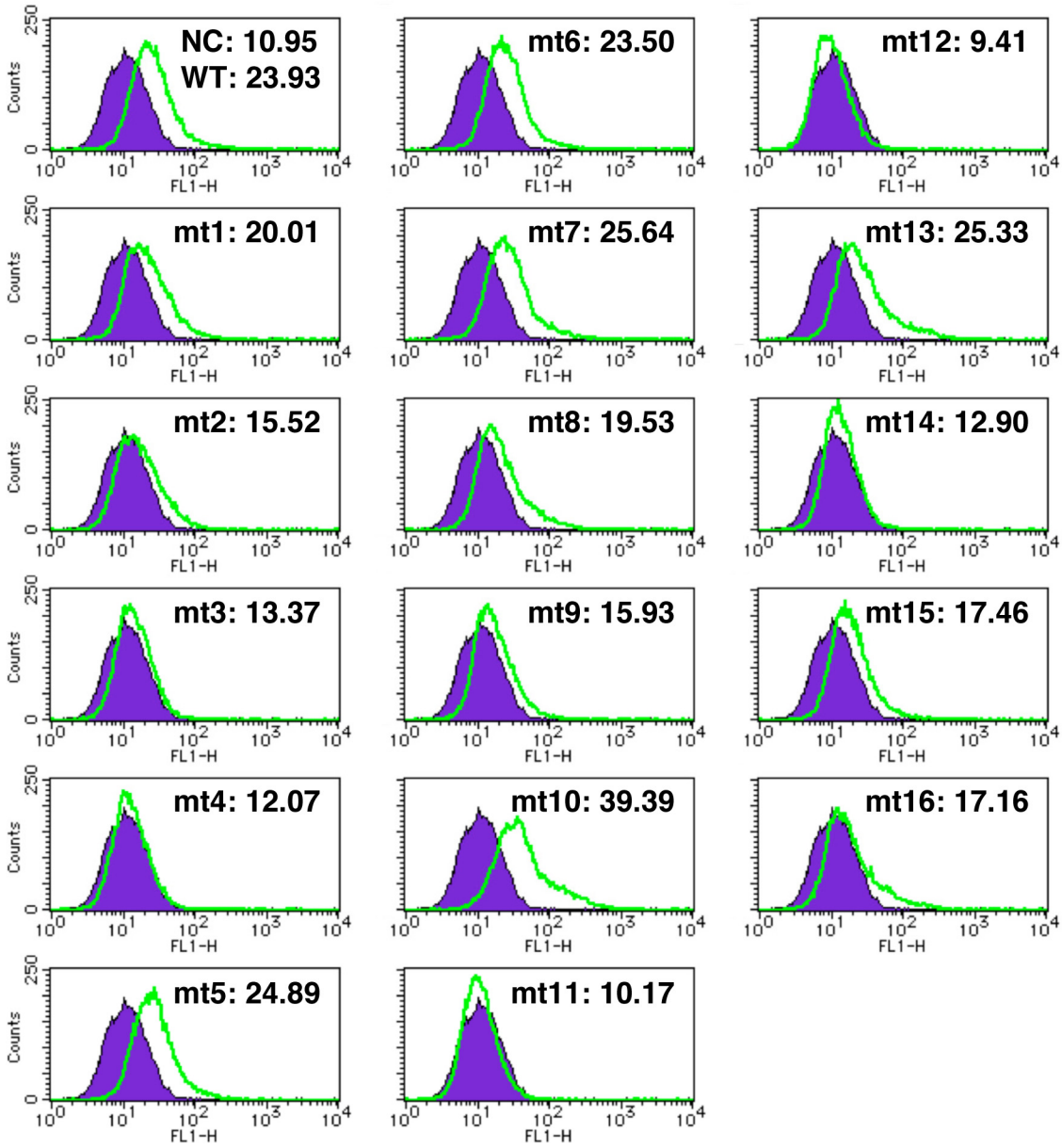

Fig. S6. Binding of HEV-LP mutants to A549 cells. Wild-type and mutant HEV-LPs (10 μg/mL) were incubated with A549 cells for 1 h at 4°C, and HEV-LP bound to cells (lined area) were detected by flow cytometry. The filled area indicates mock-incubated cells. The MFI is also indicated in each panel.

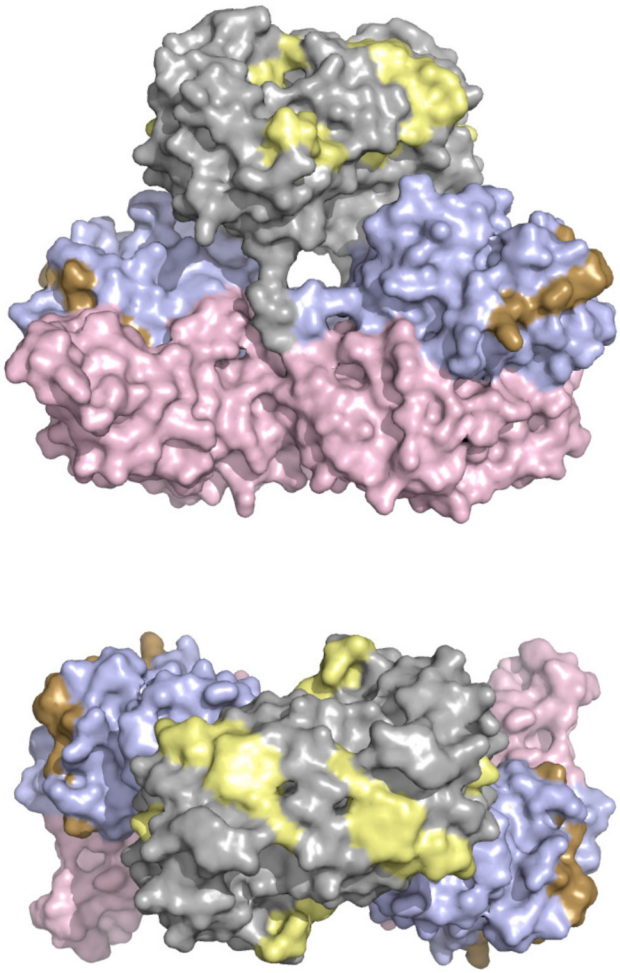

Fig. S7. Three-dimensional mapping of epitopes for neutralizing antibodies against genotype 1 strains previously reported. Surface diagrams of capsid protein dimer from a lateral (upper) or top (lower) view. The regions containing linear epitopes for the neutralizing antibodies HEV#4 and #31 (amino acids 578–607) reported by Schofield et al. (16) were colored yellow, while those of 12A10 (amino acids 423–438) and 16D7 (amino acids 423–443) reported by He et al. (13) were colored brown. Domains S, M, and P are colored pink, blue, and gray, respectively.